

Mesoscopic approach for modelling the nonlinear hysteretic response of damaged porous media in quasi-static and dynamic loading: Effects of pressure and moisture saturation

J.Carmeliet

Laboratory of Building Physics, Dept. of Civil Engineering, Faculty of Applied Science, Kasteelpark Arenberg 51, B-3001 Leuven, Belgium

K.Van Den Abeele

Interdisciplinary Research Center, Faculty of Science, K.U. Leuven Campus Kortrijk E. Sabbelaan 53, B-8500 Kortrijk, Belgium

ABSTRACT: : In this paper we describe the role of fluids in the mechanical behaviour of non-linear elastic hysteretic materials. Experiments show that the non-linear quasi-static and dynamic material behaviour primarily changes in the range of low saturation, where high fluid-solid interaction forces are present. Using the Preisach-Mayergoyz space (P-M space) model, we show that micro- to mesoscopic hysteretic entities, that cause the non-linear response, are activated with increasing saturation. The description introduces different macroscopic interaction pressures for the reversible and hysteretic elements and provides quantitative agreement with experiment. This allows us to delineate populations of mechanical elements, where moisture induced activation is most pronounced and to correlate the observations in perspective of the material composition.

1 INTRODUCTION

Much is known about the qualitative and quantitative non-linear elastic response of heterogeneous media, such as concrete, rock and other porous materials (Guyer & Johnson 1999). The most fundamental observation of non-linear elastic behaviour comes from quasi-static tests of stress versus strain. Primary characteristics of nonlinearity are: stress-dependence of the quasi-static modulus, hysteresis (dependence on stress history) and discrete memory (memory of previous maximum strain state). Also in dynamic experiments, the non-linear behaviour is found to manifest itself in a variety of manners, including stress-dependence of the dynamic modulus, amplitude dependent attenuation and resonance frequency shift when increasing the amplitude, harmonic amplitudes (generation and amplitude dependence of second and third harmonics), frequency mixing and slow dynamics (variation of modulus during wave excitation). Observation of these effects indicates the material is behaving nonlinearly.

As the mechanisms of non-linear response in hysteretic materials are not well understood yet, phenomenological models have been appealed to. A sophisticated model called Preisach-Mayergoyz space (P-M space) model (Preisach 1935, Mayergoyz 1985), that successfully describes hysteretic non-linear behaviour of rock elasticity with discrete memory, was developed in a series of papers (McCall & Guyer 1994, Guyer et al. 1995, McCall & Guyer 1996, Guyer et al. 1997). Basis of the

model is the experimental evidence that non-linear response originates within the "bond system" of the material, that includes micro-cracks, intergrain contacts, asperities, dislocations, etc. Origin, shape and behaviour of the mechanical elements may be diverse and the scale can vary from nano- to macroscopic scale. The P-M space model is based on assuming that the elastic properties of the material result from the integral response of a large number of such mechanical elements. Each element may or may not demonstrate hysteretic behaviour. The individual elements are combined for analysis for what is known as P-M space.

Recently it has become clear that fluids significantly influence the non-linear response in porous materials due to the activation of internal molecular forces (Bourbié et al. 1986, Zinszner et al. 1997, Van Den Abeele et al. in press). The increased fluid-solid matrix interaction upon wetting causes the material to soften and to swell. Simultaneously, the strength of the material reduces and the non-linear hysteretic effects increase significantly. With respect to the latter observation, it has been shown that the non-linear quasi-static and dynamic material behaviour primarily changes in the range of low saturation, which implies that the presence of moisture plays a major role in the non-linear mechanism, or in the activation of that mechanism (Van Den Abeele et al. in press)

Purpose of this paper is to understand in greater detail the role of fluids in the non-linear response of hysteretic elastic materials. Detailed analysis of the

effects of moisture on the non-linear response may tell us more about the nature of nonlinearity and explain the role of fluids in a porous medium. The rock sample in this study is Berea sandstone. First, we will illustrate quasi-static and dynamic elastic properties in the range of 0.1% to +99% water saturation. We will also show evidence from pressure vessel resonance tests taken at near zero and near 100% water saturation. In a second section, we present the P-M space construct for tracking the non-linear behaviour of rock at a particular saturation level. The important physical quantity in this description is the density distribution ρ of the mechanical elements in P-M space. We show how ρ is easily found combining quasi-static and dynamic results. In part 4, we focus on a combined theoretical and experimental prediction of the fluid-solid interaction forces that are involved in the saturation process. To this extent, we define macroscopic interaction pressures, which express the moisture effect on the density distribution ρ . The description provides quantitative agreement with experiment. This allows us to delineate populations of mechanical elements where the moisture-induced activation is most pronounced. As a final topic in the discussion, we put the observations in perspective of the material composition of Berea sandstone and try to identify the physical origin of the mechanical elements.

2 EXPERIMENTAL OBSERVATIONS

In this section, we report on the experiments at various saturation levels. Two types of experiments are performed: quasi-static and dynamic experiments.

The *quasi-static experiments* consist of uniaxial compressive tests on cylindrical samples at different degrees of saturation (S). The external pressure (σ) was raised to a predetermined maximum pressure ($\sigma=20$ MPa) and then lowered again to zero pressure. This pressure control was repeated several times until a stable hysteresis loop was attained. The stable hysteretic loops are shown in Figure 1a for different degrees of saturation. With increasing degree of saturation the hysteresis loops extend attaining higher maximal strain levels. Extent of hysteresis, characterised by the internal surface of the loop, increases with degree of saturation. The maximal strain attained in a hysteresis loop as a function of degree saturation is given in Figure 1b. We observe an initial sharp increase in the maximal strain with water saturation. The maximal strain changes very little beyond approximately 10-15% saturation. The static modulus $E_{stat}(\sigma, S) = \partial\sigma/\partial\varepsilon$ as a function of the stress for $S=100\%$ is given in Figure 1c. The modulus-stress curves for decreasing and increasing stress cross at low stress. The modulus is discontinuous at the end points of the hysteresis loop.

The *dynamic behaviour* is studied as a function of the degree of saturation (S) and external pressure (σ). We use the *impact resonance method* on cylindrical samples for extracting the dynamic behaviour at zero pressure ($\sigma=0$) (Van Den Abeele et al. in press). Measurements were taken at numerous water saturation levels between approximately 0.1-99%. The dynamic modulus $E_{dyn}(\sigma=0; S)$ is calculated from the resonance frequency peak and the measured density at each saturation level. Between 0 and 20% saturation, we see a large change in dynamic modulus (Figure 1d). The modulus changes very little beyond approximately 20-25% saturation.

The dynamic measurements as function of the confinement pressure were made in a pressure vessel at two saturation states (nearly dry and fully saturated), using the resonance method as well (Zinszner et al. 1997). These experiments are referred to as *pressure vessel resonance* experiments. In the experiments the fluid pressure was kept at the reference atmospheric pressure. The dynamic modulus $E_{dyn}(\sigma, S)$ (S being a constant saturation value) is calculated from the measured velocity and density. The dynamic modulus in dry and saturated Meule sandstone (a sandstone with the same composition and mechanical behaviour as Berea sandstone, Van Den Abeele et al. in press) as function of external stress is illustrated in Figure 1e. The results show that the material behaves more nonlinearly at full saturation (44% change in the 0-40 MPa pressure range versus 24% for dry conditions). From Figures 1d-e, we conclude that the dynamic modulus $E_{dyn}(\sigma, S)$ is a highly non-linear function of external pressure as well of degree of saturation. $E_{dyn}(\sigma, S)$ ranges from 3800 MPa at $\sigma=0$ and $S=100\%$ towards ± 25500 MPa for $\sigma \rightarrow \infty$ and $S=0$. In Figure 1c, we compare the static and dynamic modulus at full saturation ($S=100\%$). The dynamic modulus is larger than the static modulus. Note that at stress reversal points (maximum/zero stress), the dynamic and static modulus (in decreasing/increasing regime) approach to each other.

Significant observations from all these experiments are: (1) the stress-strain behaviour and the static and dynamic moduli are non-linear functions of stress; the dynamic modulus is larger than the static modulus; (2) hysteresis is characteristic of rocks; (3) the non-linear response of the rock samples changes significantly with saturation, in particular between 0% and 10-25% water saturation; the material softens and becomes more hysteretic with increasing water saturation.

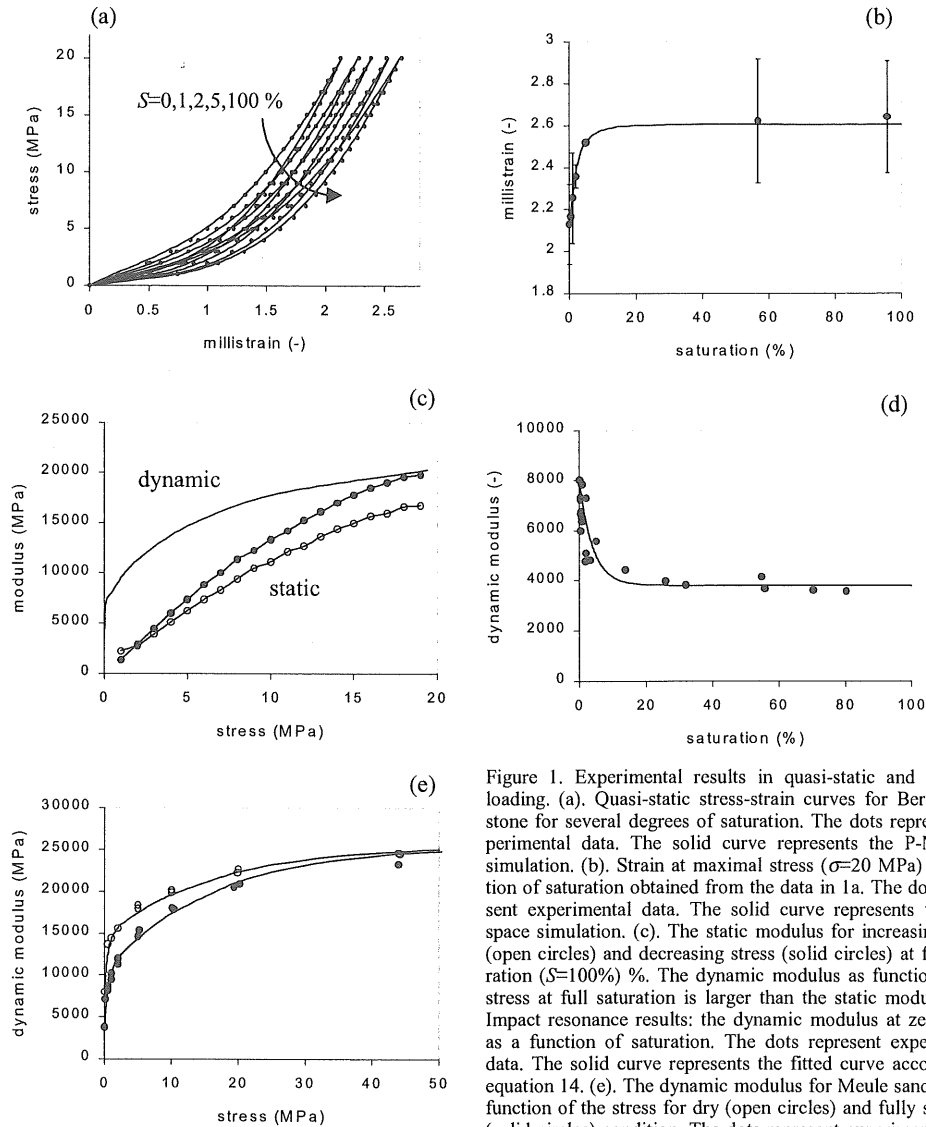


Figure 1. Experimental results in quasi-static and dynamic loading. (a). Quasi-static stress-strain curves for Berea sandstone for several degrees of saturation. The dots represent experimental data. The solid curve represents the P-M space simulation. (b). Strain at maximal stress ($\sigma=20$ MPa) as function of saturation obtained from the data in 1a. The dots represent experimental data. The solid curve represents the P-M space simulation. (c). The static modulus for increasing stress (open circles) and decreasing stress (solid circles) at full saturation ($S=100\%$) %. The dynamic modulus as function of the stress at full saturation is larger than the static modulus. (d). Impact resonance results: the dynamic modulus at zero stress as a function of saturation. The dots represent experimental data. The solid curve represents the fitted curve according to equation 14. (e). The dynamic modulus for Meule sandstone as function of the stress for dry (open circles) and fully saturated (solid circles) condition. The dots represent experimental data. The solid curve represents the fitted curve according to equations 9 for $S=100\%$ and equation 13 for $S=0\%$.

3 P-M SPACE MODEL AT CONSTANT SATURATION LEVEL

3.1 Ingredients

The fundamental reason for the hysteretic non-linear elastic behaviour is that rocks like Berea sandstone contain an enormous number of micro-, meso- or macroscopic structural features such as microcracks, macrocracks, joints, grain to grain contacts, etc. Each of these elastic units may or may not exhibit a hysteretic stress-strain behaviour. The assemblage of elements dominates the macroscopic material response, making these materials more

compressible than atomic elastic materials, and leading, in some manner or another to a larger non-linear response.

Based on the work of Preisach and Mayergoyz (Preisach 1935, Mayergoyz 1985), a phenomenological model has been developed to describe the hysteretic non-linear elastic response of rock (McCall & Guyer 1994, Guyer et al. 1995, McCall & Guyer 1996, Guyer et al. 1997). In this phenomenological material model, also called the P-M space model, the material is represented by an assemblage of elastic elements that behave hysteretic as function

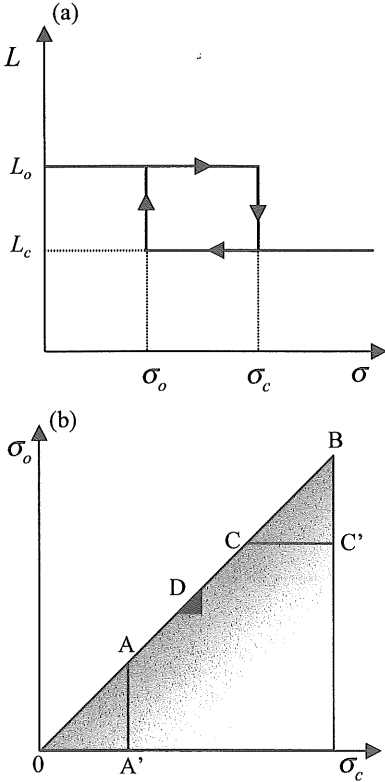


Figure 2 (a) Hysteretic Elastic Unit (HEU) in length-pressure space. (b). Typical PM-space representing the density of HEU's in a rock sample. Evolution from zero stress (point 0) to stress A produces the increasing branch of the stress-strain loop. All HEU's in the triangle 0AA' are closed at the pressure A. Following the pressure from the maximum stress B back to the stress C, we see that all the HEU's in the triangle BCC' are closed and the decreasing branch of the stress-strain loop is predicted. In a dynamic experiment, e.g. sinusoidal cycling between $\sigma_D - \Delta\sigma$ and $\sigma_D + \Delta\sigma$ (σ_D being the ambient external stress, and $\Delta\sigma$ the maximum stress excursion), one samples only a small triangle in P-M space at the point D.

of the applied stress. A single HEU (Hysteretic Elastic Unit) can only exist in one of two states, open or closed (Figure 2a). The behaviour of a HEU is such that it is originally open with length L_o , closes to obtain the length L_c as the stress increases to σ_c , and remains closed as the stress continues to increase. When the stress is decreased, the element opens at σ_o , which can be different from σ_c , returning to its original length L_o . A large number of HEU elements with differing (σ_c, σ_o) and (L_c, L_o) parameters provides a signature for heterogeneous porous material (which depends on the state of saturation and on the degree of damage of the material). We assume that the different HEU's behave independent of each other. A further simplification is made by

taking the strain $\gamma = (L_o - L_c)/L_o$ upon opening or closing of a HEU to be the same for all elements, or, γ is constant. Assuming $\gamma = (L_o - L_c)/L_o$ to be constant for all HEU's, the elements differ from another only because of the stress pair (σ_c, σ_o). The stresses σ_c and σ_o for each element can be used as the element's co-ordinates in "P-M space", with $\sigma_o \leq \sigma_c$. The density of HEU's in P-M space at constant saturation \bar{S} is given as $\rho(\sigma_c, \sigma_o; \bar{S})$. An academic example is shown in Figure 2b. Reversible elements reside on the diagonal of the σ_c - σ_o space and are described by the density distribution $\rho_d(\sigma_c = \sigma_o; \bar{S})$ ($d =$ diagonal). Hysteretic elements fill the space $\sigma_o < \sigma_c$. The density distribution of the hysteretic or off-diagonal elements $\rho_o(\sigma_c, \sigma_o; \bar{S})$ ($o =$ off diagonal) is also called the background of the P-M space. For the P-M space density distribution ρ at a given saturation \bar{S} we take

$$\rho(\sigma_c, \sigma_o; \bar{S}) = \rho_d(\sigma_c, \sigma_o; \bar{S}) \delta(\sigma_c - \sigma_o) + \rho_o(\sigma_c, \sigma_o; \bar{S}) \quad (1)$$

where δ is the delta-function. As the stress on the rock is varied, one can use P-M space to keep track of which elements are open and which are closed, and simulate the stress-strain response of the rock.

3.2 Identification of the P-M space density distribution

The diagonal density distribution ρ_d and background density distribution ρ_o at constant saturation \bar{S} are determined from dynamic and quasi-static experimental data. In a dynamic experiment, e.g. sinusoidal cycling between $\sigma - \Delta\sigma$ and $\bar{\sigma} + \Delta\sigma$ ($\bar{\sigma}$ being the ambient external stress, and $\Delta\sigma$ the maximum stress excursion), one samples only a small triangle in P-M space (triangle at stress D in Figure 2b). The dynamic properties of a material can be probed by studying the density within the triangle (Guyer et al. 1995, McCall and Guyer 1994; Van Den Abeele et al. 1997). Elements outside this "activation triangle" are left untouched. A quasi-analytical treatment of P-M space reveals that the elements on the diagonal ($\sigma_c = \sigma_o$) control the dynamic modulus $E_{dyn}(\sigma; \bar{S})$ of the material

$$E_{dyn}(\sigma; \bar{S}) = \frac{1}{\gamma \rho_d(\sigma = \sigma_c = \sigma_o; \bar{S})} \quad (2)$$

The more elements on the diagonal, the softer the material (decrease of dynamic modulus). According to equation 2, the density distribution of reversible elements on the diagonal $\rho_d(\sigma; \bar{S})$ at a given degree of saturation \bar{S} can be determined from the dynamic modulus $E_{dyn}(\sigma; \bar{S})$ determined in pressure vessel experiments. The experimental data $E_{dyn}(\sigma; \bar{S})$ are

fitted in an analytical form by a sum of exponential functions

$$E_{dyn}(\sigma; \bar{S}) = E_{dyn}(\infty, \bar{S}) - \sum_{i=1}^{n_d} a_{di}(\bar{S}) \exp(-b_{di}(\bar{S})\sigma) \quad (3)$$

where $E_{dyn}(\infty, \bar{S})$ is the limit for $\sigma \rightarrow \infty$.

The density distribution of the off-diagonal or hysteretic elements $\rho_o(\sigma_c, \sigma_o; \bar{S})$, also called background of the P-M space, determines the amount of hysteretic nonlinearity: the more elements off the diagonal, the larger the nonlinearity and the hysteresis. As most of the elements are situated near the diagonal in PM-space (Guyer et al. 1997), it is plausible to assume that the density of elements in the background decreases as one goes away from the diagonal. Let us adopt an exponential decay (Guyer et al. 1997)

$$\rho_o(\sigma_c, \sigma_o; \bar{S}) = \rho_B(\sigma_o; \bar{S}) \exp(-\kappa(\sigma_c - \sigma_o)) \quad (4)$$

where $\rho_B(\sigma; \bar{S})$ is referred to as the ‘‘basic’’ background density function and κ a decay parameter to be determined. The basic background density function is determined from quasi-static σ - ε data. Let $\Delta\varepsilon_k^\uparrow$ be the strain difference between the pressures σ_{k-1} and σ_k (where $\sigma_k = k\Delta\sigma$, $\sigma_{max} = n_k\Delta\sigma$) determined from the experimental σ - ε data as the pressure increases (\uparrow). Using the PM-model, the strain increment $\Delta\varepsilon_k^\uparrow$ is given by

$$\Delta\varepsilon_k^\uparrow = \gamma \int_{\sigma_{k-1}}^{\sigma_k} \left[\int_0^{\sigma_c} \rho(\sigma_c, \sigma_o) d\sigma_o \right] d\sigma_c \quad (5)$$

The parameter γ can be seen as a scaling constant of the strain field, and γ will inherently be incorporated in function parameters describing the density distributions of the PM-space. So, we assume $\gamma = 1$ meaning γ can be omitted in equations 2 and 5.

To determine $\rho_B(\sigma; \bar{S})$, we first assume the basic background density to be constant in the pressure range $\sigma_{k-1} - \sigma_k$

$$\rho_B(\sigma; \bar{S})|_{\sigma_{k-1} \rightarrow \sigma_k} = \bar{\rho}_{B,k}(\sigma_k; \bar{S}) \quad k = 1, \dots, n_k \quad (6)$$

where $\sigma_k = 0.5(\sigma_{k-1} + \sigma_k)$. Then, it can be shown that $\bar{\rho}_{B,k}(\sigma_k; \bar{S})$ is given by

$$\bar{\rho}_{B,k}(\sigma_k; \bar{S}) = \frac{\Delta\varepsilon_k^\uparrow - \int_0^{\sigma_k} \rho_d(\sigma_c) d\sigma_c}{\frac{\sigma_{k-1}}{\kappa} + \frac{\exp(-\kappa\sigma_k) - \exp(-\kappa\sigma_{k-1})}{\kappa^2}} \quad (7)$$

The integral in the numerator is numerically solved using quadrature formulas. The n_k values of $\bar{\rho}_B$ at the pressures σ_k are then used to approximate

$\rho_B(\sigma; \bar{S})$ in an analytical form by a sum of exponential functions

$$\rho_B(\sigma; \bar{S}) = \sum_{i=1}^{n_B} a_{Bi}(\bar{S}) \exp(-b_{Bi}(\bar{S})\sigma) \quad (8)$$

3.3 Example

We now apply the presented identification method to the experimental data at full saturation, $\bar{S} = 100\%$. The following steps are followed:

1. We first fit the dynamic modulus data, $E_{dyn}(\sigma; \bar{S} = 100\%)$, of Figure 1e using equation (3). Two exponential functions were used ($n_d = 2$). The dynamic modulus $E_{dyn}(\sigma; 100\%)$ is thus given by

$$E_{dyn}(\sigma; 100) = E_{dyn}(\infty; 100) - a_{d1}(100) \exp(-b_{d1}(100)\sigma) - a_{d2}(100) \exp(-b_{d2}(100)\sigma) \quad (9)$$

2. For a chosen value of κ , we determine, using equation (6), discrete values of the basic background density $\bar{\rho}_B$ from measured strain increments $\Delta\varepsilon_k^\uparrow$ at 20 pressure increments ($\Delta\sigma = 1 \text{ Mpa}$) of the ascending branch of the stress-strain loop. The obtained values $\bar{\rho}_{B,k}(\sigma_k; \bar{S})$ are fitted using equation (8).

3. We calculate the descending branch of the stress-strain loop. Using an optimisation procedure the value for κ is adjusted.

4. Steps 2 to 3 are repeated until the simulated and measured descending branch correspond.

Using the obtained density distributions, we simulate with the P-M space model the stress-strain curve for $\bar{S} = 100\%$, as shown in Figure 3. Comparison of experiment and simulation indicates the P-M space model is able to describe the non-linear response at constant saturation level.

4 MODELLING MOISTURE EFFECTS

4.1 Moisture induced microstresses and macroscopic modelling

Because rocks are hydrophilic materials and contain a huge specific (internal) surface area due to pore space, they exhibit intense fluid-solid interactions because of molecular and surface forces. The induced forces are known to be extremely sensitive to fluid saturation level. Solid-fluid interactions include molecular adsorption forces along pore walls, capillary pressures in capillary pores, interlayer fluid pressures due to the presence of interlayer hydrate water in nanopores. At low water saturation the microscopic fluid-solid interactions result in a compressive prestressing of the solid. As saturation increases, the compressive microstresses decrease, leading to an expansion of the material. Due to this

expansion, the dynamic mobility of the material's structural entities increases with saturation, and a reduction of the stiffness is expected. At the same time the number of elements and their ability to change states (contact – no contact; open-close; pin-unpin) increases with the degree of saturation. Therefore, an increase of non-linear elastic effects is expected at low saturation (<10-20%). At larger saturation (>20%), the effect of the microstresses levels off. In the following, we introduce a macroscopic *interaction pressure* $\pi_d(S)$ (taking compressive stress as positive), which can be considered to be representative of the combined effects of all complex fluid-solid interaction forces.

4.2 Modelling moisture influence on dynamic modulus and diagonal P-M density distribution

Let us denote the macroscopic interaction pressure, representing moisture induced microstresses causing the change of the dynamic modulus upon changes in saturation, as $\pi_d(S)$ (d meaning diagonal). We refer to $\pi_d(S)$ as *diagonal interaction pressure*, since we now that the reversible elements on the diagonal only control the dynamic modulus. We define a function f such that

$$E_{dyn}(\sigma;S) = \frac{1}{\gamma\rho_d(\sigma;S)} = f(\sigma + \pi_d(S)) \quad (10)$$

Taking full saturation as zero reference state ($\pi_d(100)=0$), we find according to equation (9)

$$\begin{aligned} f(\sigma) &= E_{dyn}(\sigma;100) = E_{dyn}(\infty;100) \\ &\quad - a_{d1}(100)\exp(-b_{d1}(100)\sigma) \\ &\quad - a_{d2}(100)\exp(-b_{d2}(100)\sigma) \end{aligned} \quad (11)$$

At dry state, equation (10) yields

$$E_{dyn}(\sigma;0) = f(\sigma + \pi_d(0)) \quad (12)$$

The value $\pi_d(0)$ can be seen as a shift of the function $f(\sigma)$ towards a higher (external) stress range and can be determined by fitting the pressure vessel resonance data $E_{dyn}(\sigma;0)$ (see Figure 1e). We found that a best fit was obtained by only shifting the first exponential function in equation (11). The general expression for $E_{dyn}(\sigma;S)$ then becomes

$$\begin{aligned} E_{dyn}(\sigma;S) &= E_{dyn}(\infty;100) \\ &\quad - a_{d1}\exp(-b_{d1}(\sigma + \pi_d(S)) - a_{d2}\exp(-b_{d2}\sigma) \end{aligned} \quad (13)$$

where we used $a_{di}(100) \equiv a_{di}$, $b_{di}(100) \equiv b_{di}$. The diagonal density distribution can easily be found using equation (10).

We still have to identify the interaction pressure $\pi_d(S)$. In order to derive an expression for $\pi_d(S)$, we use the impact resonance data $E_{dyn}(0;S)$ for different degrees of saturation at zero pressure ($\sigma=0$) (see Figures 1d). To do so, we first fit the experimental

impact resonance data $E_{dyn}(0;S)$ by an exponential expression

$$\begin{aligned} E_{dyn}(0;S) &= E_{dyn}(0;100) + \\ &\quad (E_{dyn}(0;0) - E_{dyn}(0;100))\exp(-b_S S) \end{aligned} \quad (14)$$

The fitting parameters are summarised in Table 1. According to equations (13) and (14), we can write for $E_{dyn}(0;S)$ at zero pressure as a function of S

$$\begin{aligned} E_{dyn}(0;S) &= E_{dyn}(0;100) \\ &\quad + (E_{dyn}(0;0) - E_{dyn}(0;100))\exp(-b_S S) \\ &= E_{dyn}(\infty;100) - a_{d1}\exp(-b_{d1}\pi_d(S)) - a_{d2} \end{aligned} \quad (15)$$

which leads to the following expression for $\pi_d(S)$

$$\begin{aligned} \pi_d(S) &= \\ &\quad - \frac{1}{b_{d1}} \ln \left(1 - \frac{(E_{dyn}(0;0) - E_{dyn}(0;100))\exp(-b_S S)}{a_{d1}} \right) \\ &\quad \approx \frac{(E_{dyn}(0;0) - E_{dyn}(0;100))\exp(-b_S S)}{a_{d1}b_{d1}} \end{aligned} \quad (16)$$

We note that the function $\pi_d(S)$, has approximately an exponential shape with the same decay constant (b_S) as for the exponential dependence of the dynamic modulus on the saturation, $E_{dyn}(0;S)$. The maximal value of $\pi_d(S)$ is attained at $S=0$ and is found to be 5.14 MPa.

4.3 Modelling moisture effect on background P-M density distribution

To determine the dependence of the background density $\rho_o(\sigma_c, \sigma_o;S)$ on saturation, we follow the identification procedure for $\rho_o(\sigma_c, \sigma_o;S)$ as presented in 3.2. The stress-strain data at seven different values of the saturation were considered: $\mathcal{S}_j = 100, 60, 5, 2, 1, 0.5$ and 0% (see e.g. Figure 1a). We assume the decay parameter κ to be independent on the saturation level. The basic background density function $\rho_B(\sigma; \mathcal{S}_j)$ for each saturation level \mathcal{S}_j is then approximated by a sum of three exponential function ($n_B=3$ in equation 8) and the parameters $a_{Bj}(\mathcal{S}_j)$ and $b_{Bj}(\mathcal{S}_j)$ ($i=1..3, j=1..7$) are determined based on the discrete data $\rho_{Bk}(\sigma_k; \mathcal{S}_j)$ ($k=1..20$). We found the constant $a_{Bj}(\mathcal{S}_j)$ of the first exponential function in equation 8 to be highly dependent on the saturation level, while the other parameters were found to be merely insensitive to the saturation level. Let us define the macroscopic interaction pressure, representing moisture induced microstresses responsible for the change of the basic background density upon changes in saturation, by $\pi_B(S)$ (B meaning background density). In analogy to the exponential dependence of the diagonal interaction pressure $\pi_d(S)$ on saturation (equation 16), we assume an exponential relation for the *background interaction pressure*

$$\pi_B(S) = a_{\pi B} \exp(-b_{\pi B} S) \quad (17)$$

Since only the first exponential function is found to be dependent on saturation, we may write, in analogy to expression 13 for the diagonal density distribution, the general expression for the basic background density function $\rho_B(\sigma; S)$ as

$$\rho_B(\sigma; S) = a_{B1} \exp(-b_{B1}(\sigma + \pi_B(S))) + a_{B2} \exp(-b_{B2}\sigma) + a_{B3} \exp(-b_{B3}\sigma) \quad (18)$$

Note that the maximal value of the background interaction pressure $\pi_B(S)$ is attained at $S=0$ and is found to be 1 Mpa, which is much lower compared to the diagonal interaction pressure ($\pi_d(0) = 5.14$ MPa).

In order to check the validity of the determined diagonal and background density distribution and their dependence on saturation, we simulate the hysteresis loops for different saturation levels and the dependence of the strain at maximal pressure on saturation (see Figure 1a-1b). A good agreement between experimental results and P-M simulations is observed, showing the ability of the P-M space model, enriched with moisture interaction pressures, to describe the experimental findings.

4.4 Discussion

We observed that only the first exponential function of the diagonal as well as the first exponential function of the background density distribution is sensitive to moisture. The first exponential function describes HEU's, which open and close at low external pressure. This population of HEU's is thus found to be moisture sensitive. On the other hand, the HEUs, which open and close at higher external pressure, are found to be insensitive to moisture. We can thus distinguish two different populations of HEU's in Berea sandstone: a first population sensitive to moisture situated in the lower pressure range and a second population at high opening and closing pressure, which are insensitive to moisture.

Referring to the P-M space, we interpret the moisture sensitivity as follows: in a wet state the same excursion in external stresses is able to activate more HEU's of the first population than in a dry state. The activation results in a larger density of HEU's in an activation triangle, and therefore a lower modulus and higher nonlinearity. This means that partial saturation induces a shift in the distribution of certain elastic elements in the P-M space towards a higher (external) stress range compared to the reference fully saturated state. The total number of elastic elements in P-M space is assumed conserved. Only the number of activated units increases with saturation.

The moisture dependence, described by the macroscopic interaction pressures $\pi_d(S)$ and $\pi_B(S)$, turns

out to be only important in the low saturation range, between 0 and 20 %. Moreover, the interaction pressure for the reversible elements $\pi_d(S)$ is found to be 5 times larger compared to interaction pressure for the hysteretic elements $\pi_B(S)$. Reversible elements of the first population are thus more moisture sensitive than hysteretic elements.

In (Van Den Abeele et al. in press), we used the equivalent macroscopic capillary pressure p_c ($p_c = p_g - p_l$; p meaning pressure and subscripts g and l referring to gaseous and liquid phase) as a physically more relevant potential to describe the state of the fluid phases present in the porous medium. Using the state relation $S(p_c)$ (Carmeliet et al. 1999) we express the interaction pressures $\pi_d(S)$ and $\pi_B(S)$ as function of the capillary pressure. Relating capillary pressure to pore size (using Laplace's law), we find that only moisture present in the finer pores (10^{-9} - 10^{-6} m) is responsible for the observed moisture effect on the non-linear elastic behaviour of rock (Figure 4). Moisture present in the midsize pore system (peak around 10^{-5} m) is found to play a negligible role in the material behaviour of Berea sandstone.

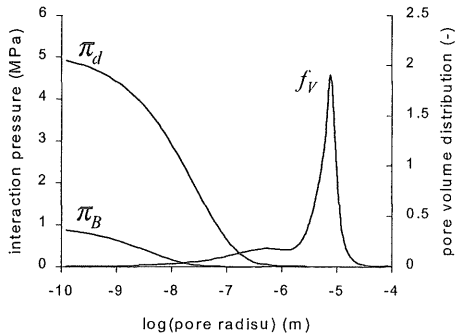


Figure 4. The diagonal interaction pressure $\pi_d(S)$ and background interaction pressure $\pi_B(S)$ as function of the equivalent pore radius. The pore volume distribution f_V of Berea sandstone indicates that only the fine pore system produces the interaction pressures.

As a final remark, we try to link our observations to the material composition of Berea sandstone. Berea sandstone is composed of quartz grains and contains a considerable amount of clay and other secondary mineralisation. The bonding material is primarily silica. Based on all observations, we think that especially the fine pores, situated in the soft material (clay, silica glue), are responsible for the observed moisture influence. Also, the HEU's of the first population are assumed to be situated in this soft material and are therefore easily activated by moisture present in the fine pore system. The second population of HEU's, which are closing and opening at higher pressures, are thought to be represented by structural features of larger size: grain-to-grain boundaries, asperities and microcracks. Moisture

present in these features only produce low capillary pressures, which explains the moisture insensitivity of the second population of HEU's.

5 CONCLUSIONS

The experiments we described in this paper suggest evidence for the role of fluids on the non-linear behaviour of Berea sandstone. We conducted both quasi-static and dynamic measurements. Significant observations from these experiments were: the non-linear response of the rock samples changes significantly with saturation, in particular between 0% and 10-25% water saturation; the material softens and becomes more hysteretic with increasing water saturation.

The non-linear hysteretic behaviour is interpreted using the so-called P-M space model. In this phenomenological material model, the material is represented by an assemblage of elastic elements that may or may not behave hysteretic as function of the applied stress. The important physical quantity in this description is the density distribution of the HEU's (Hysteretic Elastic Units) in P-M space. Reversible elements are described by the diagonal density distribution, while hysteretic elements are described by the background density distribution. We proposed to describe the density functions by a sum of exponential functions, which simplifies the identification problem and offers the possibility to discern different populations of HEU's.

To incorporate moisture effects in the classical P-M construct, we enriched the P-M space model by moisture interaction pressures, which represent the combined effects of all complex fluid-solid interaction forces. The moisture interaction pressure for reversible elements is found to be larger compared to hysteretic elements. The interaction pressures induce a shift of elements in P-M space and moisture induced effects can thus be interpreted as a relocation in the density of HEU's in the P-M space. The observed decrease of the dynamic stiffness with increasing saturation can be interpreted as an increase of the reversible elements. At the same time, the increase of nonlinearity points towards an increase of the number of hysteretic elements.

Based on the P-M modelling, we can distinguish two different populations of HEU's in Berea sandstone: a first population sensitive to moisture situated in the lower pressure range and a second population at high opening and closing pressure, which are insensitive to moisture. Reversible elements of the first population are found to be much more moisture sensitive compared to hysteretic elements. Linking these observations with the material structure of Berea sandstone, we think that especially the fine pores, situated in the soft material between the sand

grains are responsible for the observed moisture influence. The HEU's of the first population are assumed to be situated in this soft material and are therefore easily activated by moisture present in the fine pore system. The second population of HEU's, which are closing and opening at higher pressures, are thought to be represented by structural features of larger size: grain-to-grain boundaries, asperities and microcracks. Moisture present in these features only produce low capillary pressures, which explains the moisture insensitivity of the second population of HEU's.

In conclusion, we believe that the phenomenological P-M model offers a great potential for understanding the complex non-linear hysteretic elastic behaviour of porous materials including the effect of moisture saturation and damage. Though limited in its present state to applications for rocks, the model will be applied to cementitious materials like concrete in the near future.

REFERENCES

- Bourbié, T., Coussy O., & Zinszner B. 1986 *Acoustique des milieux poreux*. Paris: Editions Technip.
- Carmeliet, J., Houvenaghel, G. & Descamps, F. 1999. Multiscale network for simulating liquid water and water vapour transfer properties of porous materials. *Transport in Porous media*, 35: 67-88.
- Guyer, R.A., & Johnson, P.A. 1999. Nonlinear mesoscopic elasticity: Evidence of a new class of materials. *Physics Today* 52: 30-35.
- Guyer, R. A., McCall, K. R. & Boitnott, G. N. 1995. Hysteresis, discrete memory and nonlinear wave propagation in rock. *Phys. Rev. Let.* 74: 3491-3494.
- Guyer, R. A., McCall, K. R., Boitnott, G. N., Hilbert Jr., L.B. & Plona, T.J. 1997. Quantitative implementation of Preisach-Mayergoyz space to find static and dynamic elastic moduli in rock. *J. Geophys. Res.* 102: 5281-5293.
- Mayergoyz, J.D. 1985. Hysteresis models from the mathematical and control theory points of view. *J. Appl. Phys.* 57: 3803.
- McCall, K. R. & Guyer, R. A. 1994. Equation of state and wave propagation in hysteretic nonlinear elastic material. *J. Geophys. Res.* 99: 887-23,897.
- McCall, K. R. & R. A. Guyer. 1996. A new theoretical paradigm to describe hysteresis, discrete memory and nonlinear elastic wave propagation in rock. *Nonlinear Processes in Geophysics* 3: 89-101.
- Preisach, F. 1935. Über die magnetische Nachwirkung. *Z. Phys.* 94: 277.
- Van Den Abeele, K. E-A., Johnson, P. A., Guyer, R. A. & McCall, K. R. 1997. On the analytical solution of hysteretic nonlinear response in elastic wave propagation. *J. Acoust. Soc. Am* 101: 1885-1898.
- Van Den Abeele, K E-A., Carmeliet, J., Johnson P.A. & Zinszner, B. In press. The Influence of Water Saturation on the Nonlinear Elastic Mesoscopic Response in Earth Materials, and the Implications to the Mechanism of Nonlinearity, *J. Geophys. Res.*
- Zinszner B., Johnson PA and Rasolofosaon P.N.J. 1997. Influence of change in physical state on elastic nonlinear response in rock: effects of confining pressure and saturation. *J. Geophys. Res.* 102: 8105-8120.